Rejection of partial-discharge-induced pulses in fission chambers designed for sodium-cooled fast reactors

H. HAMRITA*[1], C. JAMMES[2], G. GALLI[1], F. LAINE[1]

[1]CEA, LIST, Sensors and Electronics Laboratory, 91191 Gif-sur-Yvette, France.
[2]CEA, DEN, DER, Instrumentation, Sensors and Dosimetry Laboratory, Cadarache, F-13108 Saint-Paul-lez-Durance, France.

Abstract

Under given temperature and bias voltage conditions, partial discharges can create pulses in fission chambers. Based on experimental results, this phenomenon is in-depth investigated and discussed. A pulse-shape-analysis technique is proposed to discriminate neutron-induced pulses from partial-discharge-induced ones.

Keywords: Sodium fast reactor. Neutron detection. High Temperature Fission Chamber. Partial Discharge. Pulse shape analysis

I. INTRODUCTION

FAST neutron sodium-cooled reactors (FSR or SFR for Sodium-cooled Fast Reactor) are one of the advanced reactors selected by the Generation IV International Forum.

Fission chamber has been identified as the most suitable neutron detector to be used in the vessel of a sodium fast reactor [1-3]. This detector namely High Temperature Fission Chamber (HTFC), must be able to operate under high irradiation up to 10^{10} n/cm².s and high temperature up to 650°C. One of the effect of this hostile environment is the superposition of a partial discharge signal to the useful signal measured with a fission chamber. Theoretical studies have defined the phenomenon of partial discharges (PD) in gases and solids. Indeed, partial discharges occurring in the gas are known as "Corona partial discharges" [4], whereas partial discharges occurring in solids are called "electronic avalanche" [5] [6]. In this paper, we show experimental results obtained with three HTFC at different values of temperature and bias voltage, under neutron beam irradiation and off beam.

This paper is organized as follows: in Section 2, an overview of the methodology used to carry out these tests is presented. In Section 3, results off beam will be shown. In Section 4, results of beam tests will be presented, discussed, and compared to those off beam.

II. EXPERIMENTAL DETAILS

Our objective is to understand what are the operational conditions, mainly in terms of temperature and bias voltage. Indeed, these two parameters could be the cause of partial discharges in HTFC. Three identical chambers are tested. All of them are placed together in a tubular furnace which can reach a temperature of 650 ° C. Temperature is increased gradually. Several types of electronics and outputs were used for collecting and processing the signal obtained from PD and neutron pulses. Each HTFC was coupled to a CANBERRA 7820 amplifier. This module has two outputs: an analog output and a logic output (TTL). Whereas TTL signal allows for characterizing arrival time distribution of the observed pulses, analog signal allows for investigation of their shape and amplitude. The amplifier was controlled through the GENIE 2000 CANBERRA software. The TTL output is connected to both a standard counter/timer and the PING time-stamping acquisition system, developed at the French Atomic Commission (CEA) [7]. The PING instrumentation allows for measuring the time elapsed between two subsequent pulses. Pulses (analog output) measurements are performed with a large bandwidth digital oscilloscope (20 giga-samples/s, 10 bits). A block diagram of the experimental setup is shown in Fig. 1.

Tests under irradiation have been performed at the SAPHIR facility [8] which is located at CEA in Saclay (France). The SAPHIR facility houses two electron accelerators. A 15 MeV electron accelerator has been used as a neutron source for these experiments. Neutrons, known as photoneutrons are produced by photonuclear reactions in the target of the accelerator [9]. A target made of tantalum has been used for these experiments. Maximum neutron fluence is about 10^7 n/cm².s. The gamma dose rate is about 10 Gy/hour. The same electronics were used to perform the beam tests and off beam.

Characteristics of the three HTFCs are similar and are given in Table 1. In the following, the three HTFC will be named A, B and C.

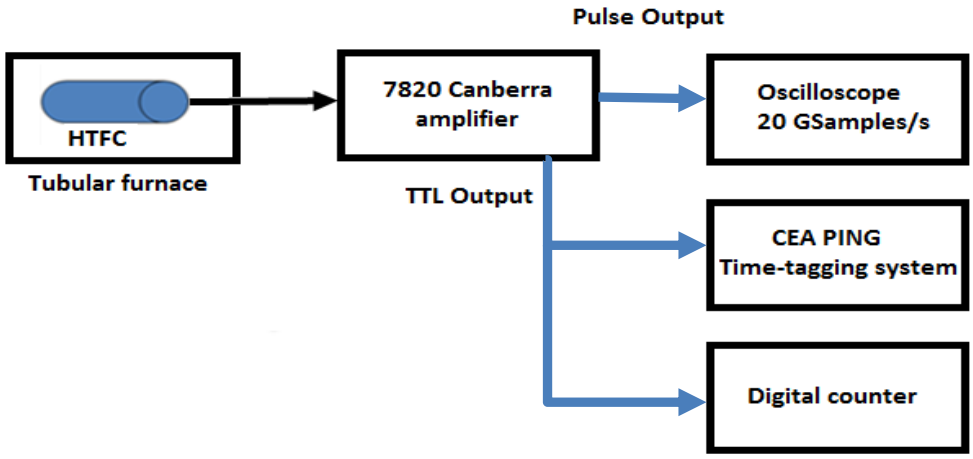

Fig. 1. Experimental setup

Table 1: Nominal outer diameter D; active length of the fissile material L; insulator material I; filling gas G; pressure P; fissile material F.

D	L	I	G	P	F
7 mm	12 cm	Alumina	Argon	900 kPa	^{235}U

Before starting measurements at high temperature, we verified that the HTFCs, labelled A, B and C, used for these experiments, correctly operate at room temperature under neutron flux. Figure 2 shows the so-called discrimination and saturation curves [11]. These are counts versus discrimination level for the first curve and versus bias voltage for the second one. From this figure, we find that the 3 chambers appear to operate as expected and provide similar output signals. The shape of the curves is representative of typical curves of a fission chambers [12]. Discrimination curves show that to detect all neutrons we have to set a threshold between 400 mV and 600 mV. Saturation curves obtained at threshold of 400 mV, show that we can use all the HTFCs with a bias voltage up to 800 V without risk to have an avalanche effect .

At room temperature and without neutron flux, the counter counts for several minutes zero pulse at threshold of 400 mV and at different bias voltage up to 800 V. We conclude that at room temperature it has no partial discharge.

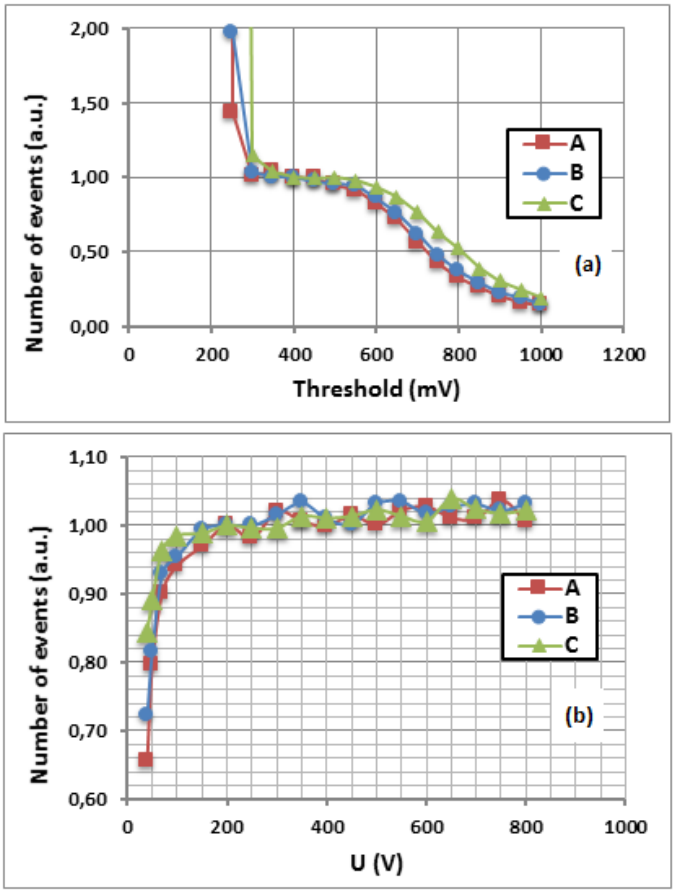

Fig. 2. Proof of normal operation at room temperature
(a) Discrimination curve. (b) Saturation curve.

III. OFF BEAM TEST RESULTS

A. Measurement of partial discharge count rate

In order to discriminate between PD pulsess of those from neutrons in fission chambers , we need to know their abort count rates and their appearance law. According to reference [13] , the occurrence of PD in the air depends on the pressure and temperature. In our case the gas isn't the air but the argon.

In this section, we present the number of PDs according to the supplied voltage obtained at different temperatures. Fig. 3, Fig. 4 and Fig. 5 show results obtained with HTFC A, B and C, respectively. For each pair of temperature (T) and bias voltage (U), pulse counting is performed within 100 seconds.

We find that the number of partial discharges increases with the supply voltage and temperature. It reaches 20 events per second for the pair (650 ° C, 300 V) for HTFC A and B and 100 events per second for HTFC C at 600°C and 400 V.

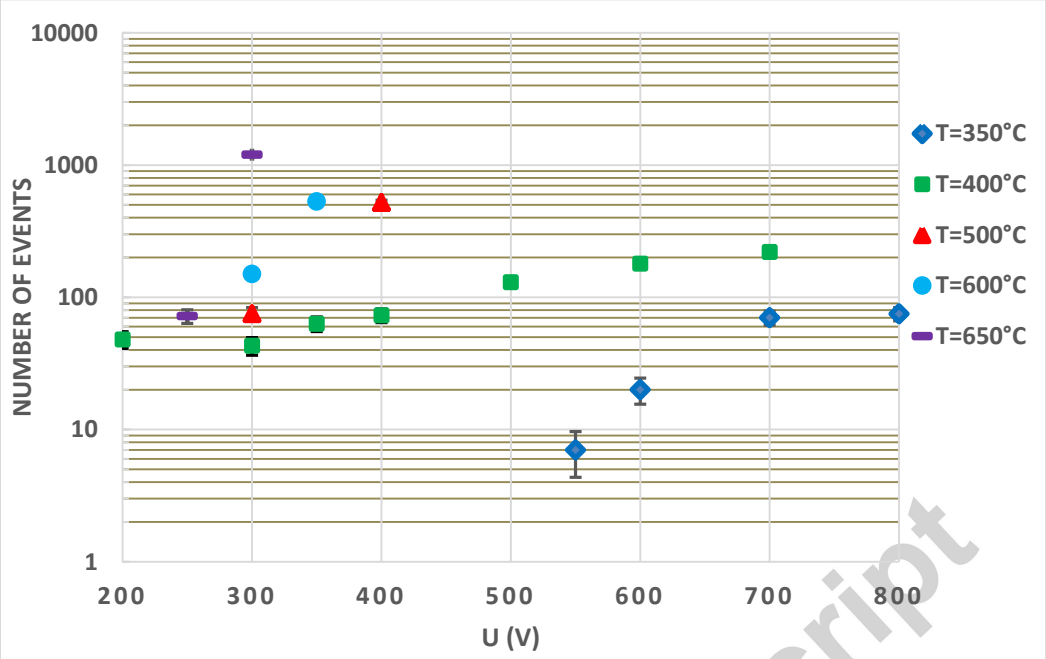

Fig. 3. Measurement of PD counting rate according to the supply voltage, at different temperature values for the HTFC A.

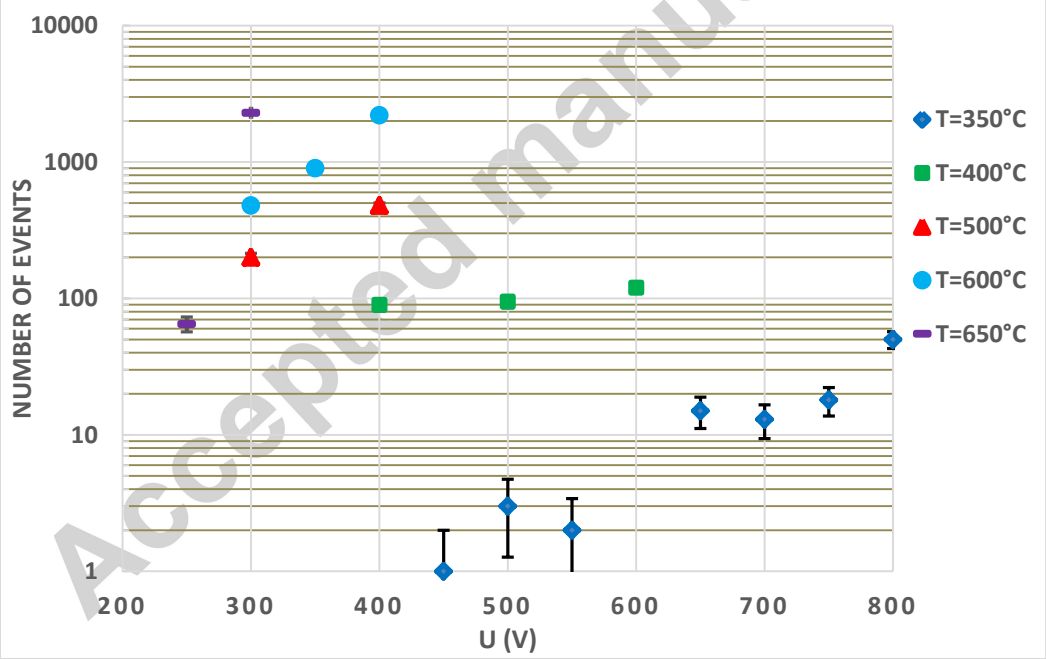

Fig. 4. Measurement of PD counting rate according to the supply voltage, at different temperature values for the HTFC B.

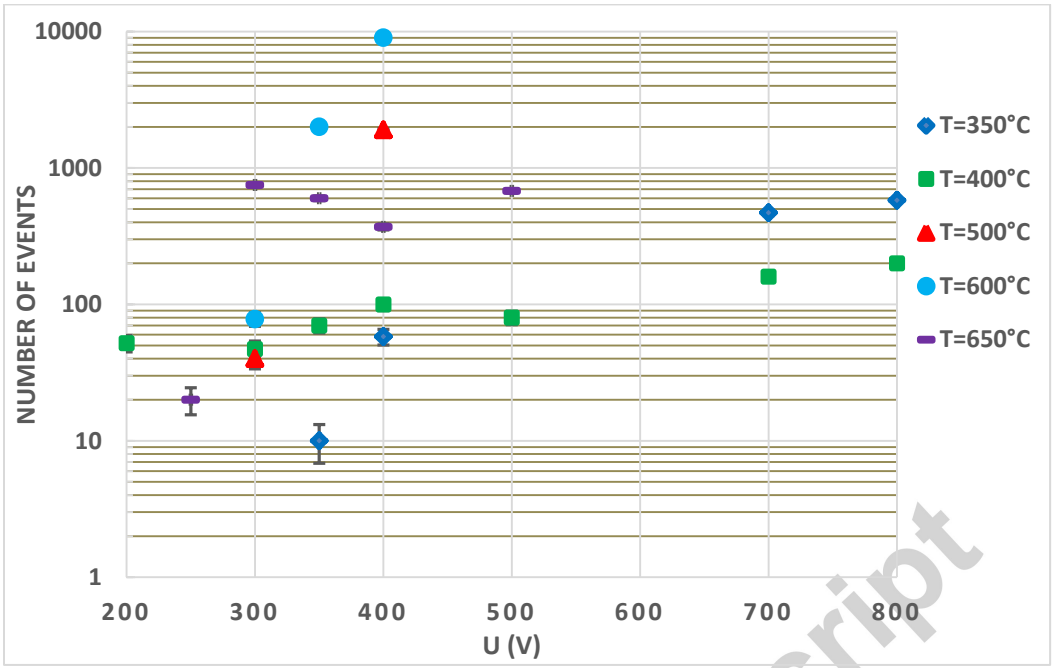

Fig. 5. Measurement of PD counting rate according to the supply voltage, at different temperature values for the HTFC C.

Although HTFC A, B and C are manufactured according to the same industrial process, it comes that they differently behave at high temperature. Figures 3, 4 and 5 show their PD occurrences are noticeably different. At the moment, we can not explain what causes this variable behavior. One can only assume that the present industrial process plays an important role in the PD appearance at high temperature. In addition, one can also note that, especially in the HTFC A and C, lower voltage PD not occur at the maximum temperature (650°C), but rather at 400°C, which leaves us suppose that the physical processes that lead to the generation of PD is not strictly linear with temperature.

B. Arrival time distribution of partial discharges

In order to obtain the distribution of PD arrival times, we used the PING instrumentation, which time-stamps pulses with a time resolution of 20 ns. Fig. 6 shows graphs of subsequent periods (Delta-T) between PD-induced pulses measured for various pairs (temperature, bias voltage) applied to HTFC B and zero in x-axis is relative to the moment the bias voltage is switched on. We also tried to find laws that describe the behavior of the HTFC for each temperature and bias voltage. Table 2 shows different parameters of the fitting analytical models. The results obtained with the other detectors are similar but with different parameter values.

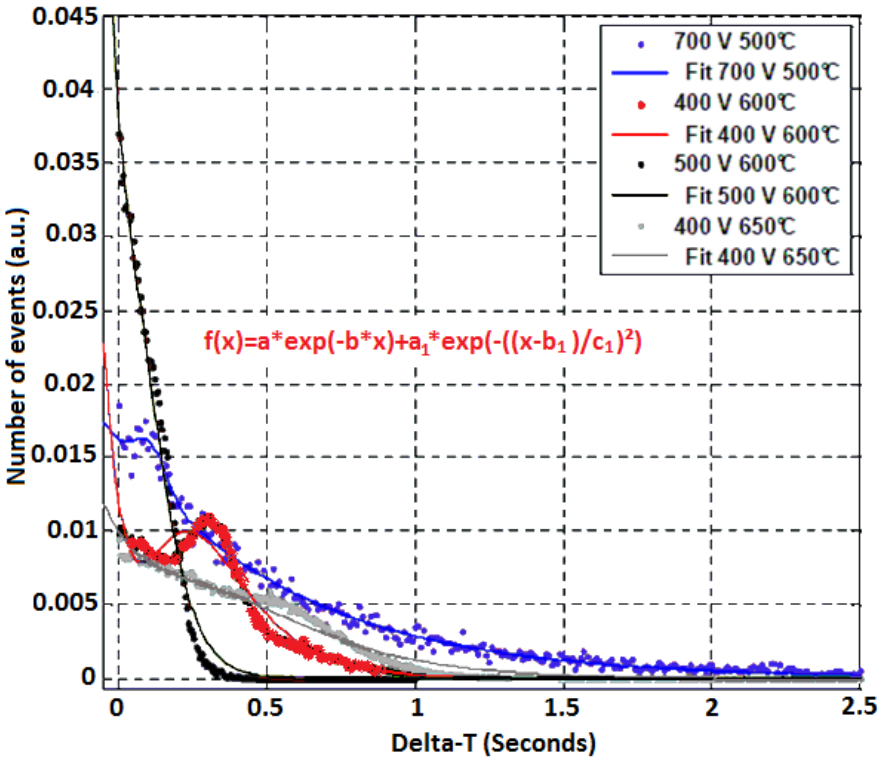

Fig. 6. Arrival time distributions of PDs observed in HTFC B for various temperature-voltage pairs.

Table 2: Double-exponential fitting model and its estimated parameters.

T (°C)	U (V)	a	b	a1	b1	c1
500	700	0,016	1,705	0,003	0,108	0,074
600	400	0,072	5,535	-0,086	-0,16	-0,267
600	500	0,154	13,7	-0,863	-0,257	0,181
650	400	0,034	3,28	-0,0574	-0,509	-0,549

These results show that after a fast transient that appears at the beginning of bias voltage, the partial discharge time occurence is exponentially distributed. Given that neutron-induced pulses follow the same time behavior, the two pulse types cannot be discriminated using sort of time-based techniques.

C. Signal analysis of partial discharges

For both various temperatures and bias voltages, PD-induced pulses were acquired using an oscilloscope. Fig. 7 and Fig. 8 show pulses obtained with HTFC A and B at 600°C and 400 V, respectively.

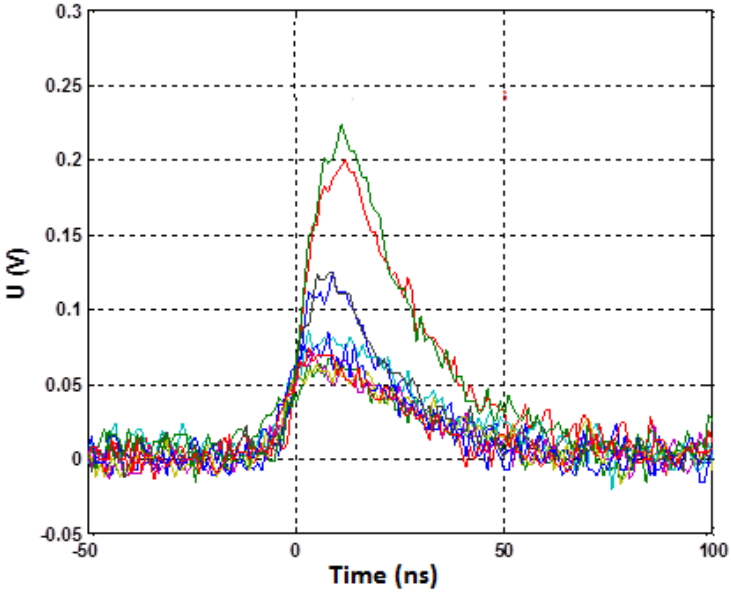

Fig. 7. PD-induced pulses obtained with HTFC A.

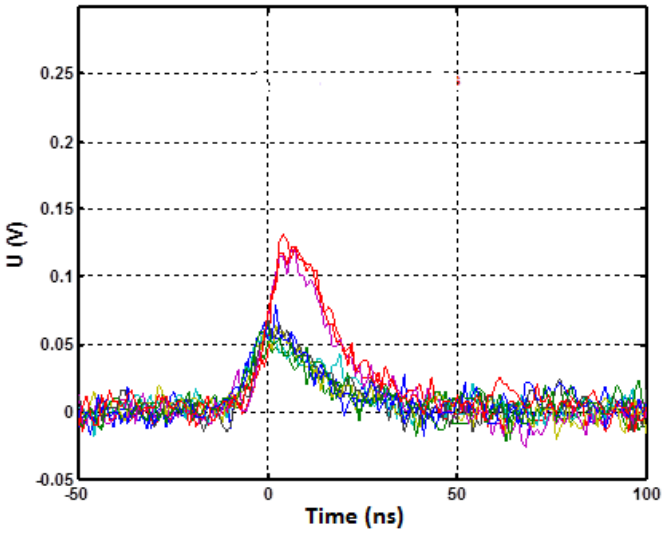

Fig. 8. PD-induced pulses obtained with HTFC B.

In first time we can note that amplitudes of the PD-induced pulses vary significantly. This may be accounted for by the fact that the pulse shapes are likely to depend on the location inside the HTFC itself, where PDs are created, and on the amount of released charges. Another striking observation is that the pulse FWHM is almost constant. Indeed, Fig. 9 displays the FWHM distribution of about 10^4 PD-induced pulses obtained with HTFC A at 600°C and 400V. This distribution shows a FWHM about 30 ns.

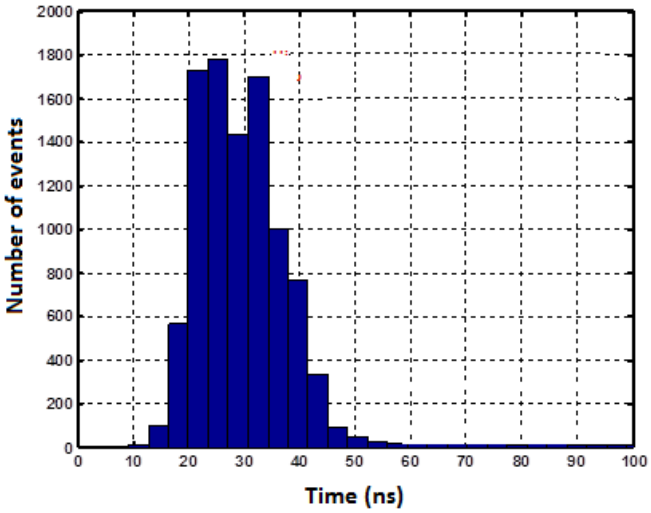

Fig. 9. FWHM distribution of PD-induced pulses obtained with HTFC A.

IV. BEAM TEST RESULTS

A. Signal analysis of neutron pulses at room temperature

In this section, we compare neutron and PD-induced pulses and from a qualitative point of view, pulses induced by either neutrons or PDs look very similar. First, it was necessary to measure neutron pulses only. This was carried out at room temperature. At this temperature, no PDs were observed with the three HTFCs. Fig.10 presents a few neutron-induced pulses obtained with HTFC C. It shows that neutron-induced pulses exhibit various amplitudes. This comes from the various energy released by fission products created in the fissile layer of the chamber. However, we can note that the variation in width of the neutron-induced pulses is rather limited. Fig. 11 and Fig. 12 illustrate amplitude and FWHM distributions, respectively, obtained from about 10^4 neutron pulses using HTFC C operating at room temperature. We note that mean FWHM value is about 90 ns.

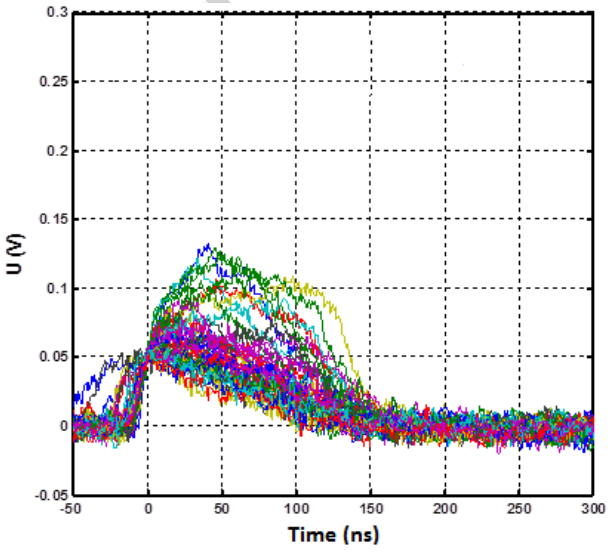

Fig. 10. Neutron-induced pulses obtained with HTFC C at room temperature.

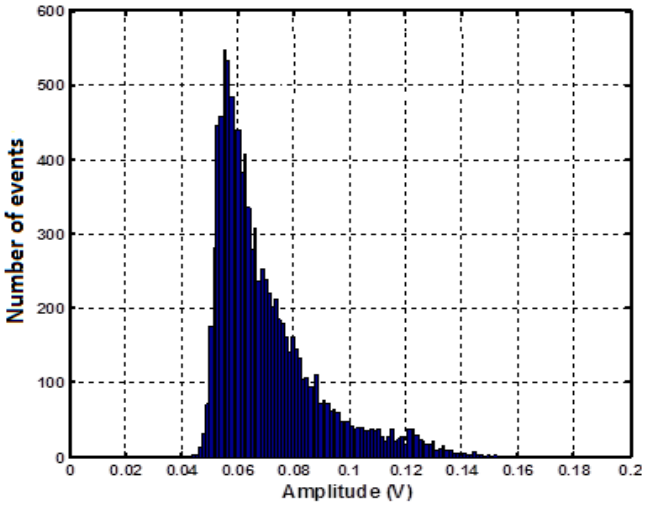

Fig. 11. Amplitude distribution of neutron-induced pulses obtained with HTFC C.

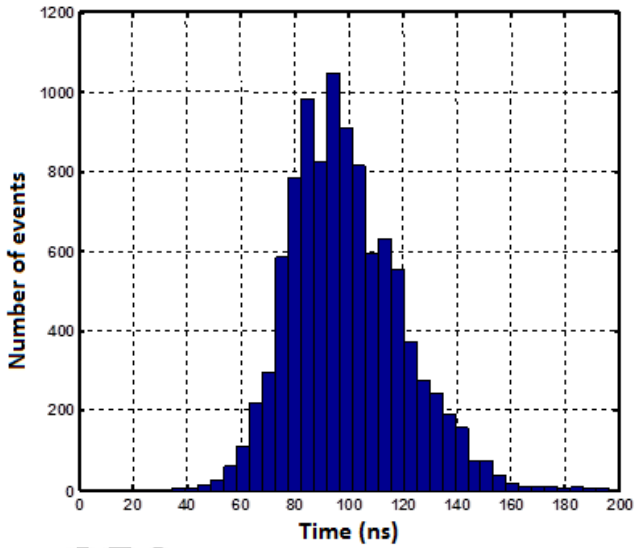

Fig. 12. FWHM distribution of neutron-induced pulses obtained with HTFC C.

B. Signal analysis of neutron pulses at different temperature values

In this section, we compare FWHM distributions of neutron-induced pulses obtained with HTFC B taken at different temperature values. Fig. 13 clearly shows that the FWHM distribution doesn't change appreciably when we increase the temperature between 20°C and 650°C. This would lead to state that the mobility of the ions remains constant when the gas temperature varies, so this would lead to go against the theory because the theory of mobility of ions in gas implies that the mobility of ions decreases when the gas temperature rises [14]. But this is true only for the ions ionized one time and for monatomic ions while different theories, backed up with some experiences, are currently being studied for ions ionized several times and for diatomic ions [14].

So by reason of the moderate increase temperature, without direct ionization effects, and for the unknown type of ions present in the HTFC, we base our conclusions on the experimental data in Fig. 13 which shows, as mentioned at the beginning of this section, that the FWHM distribution doesn't change appreciably when we increase the temperature between 20°C and 650°C.

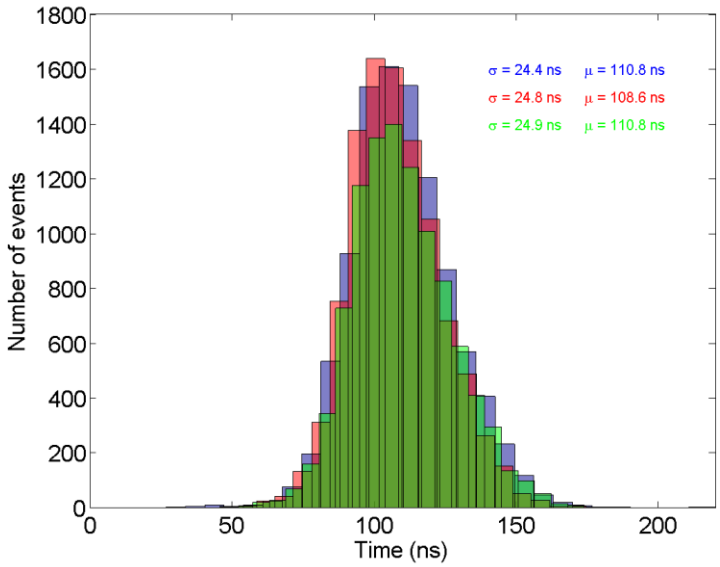

Fig. 13. FWHM distribution of neutron-induced pulses obtained with HTFC B at 200°C (blue), 400°C (red) and 600°C (green).

C. Experimental rejection of partial discharges

At high temperature (600°C), in the presence of PD-induced pulses, HTFC C was irradiated under neutron flux. We plotted amplitude and FWHM distributions of a set of about 10^4 acquired pulses. Fig. 14 clearly shows that it is not easily to distinguish between neutron and PD-induced pulses using the pulse amplitude as a criterion. Indeed, in both cases, amplitudes vary between 40 mV and 300 mV. On the contrary, the FWHM distribution displayed in Fig. 15 reveals two well-separated peaks. The left peak is accounted for by the PD-induced pulses: the corresponding distribution is very similar to the one obtained off beam (Fig. 9). The right peak comes from neutron-induced pulses: the corresponding distribution is very similar to the distribution obtained at room temperature (Fig. 12). This undoubtedly shows that the FWHM criterion allows for a successful discrimination between the two types of pulses.

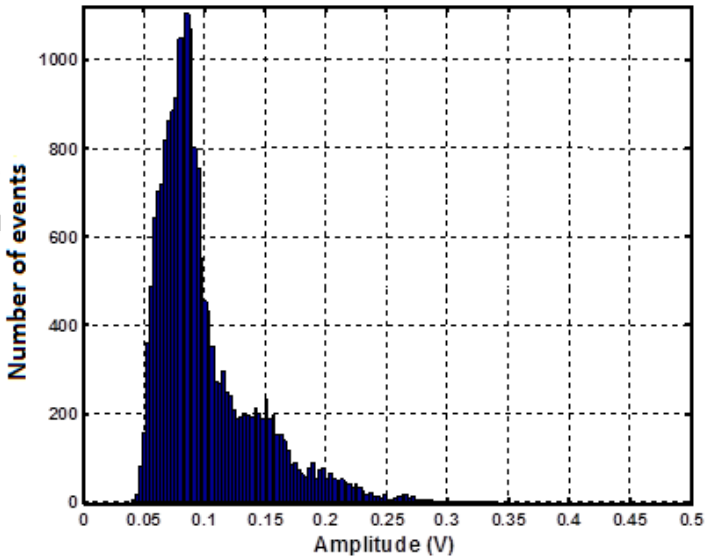

Fig. 14. Amplitude distribution of both neutron and PD-induced pulses obtained with HTFC C at 600°C.

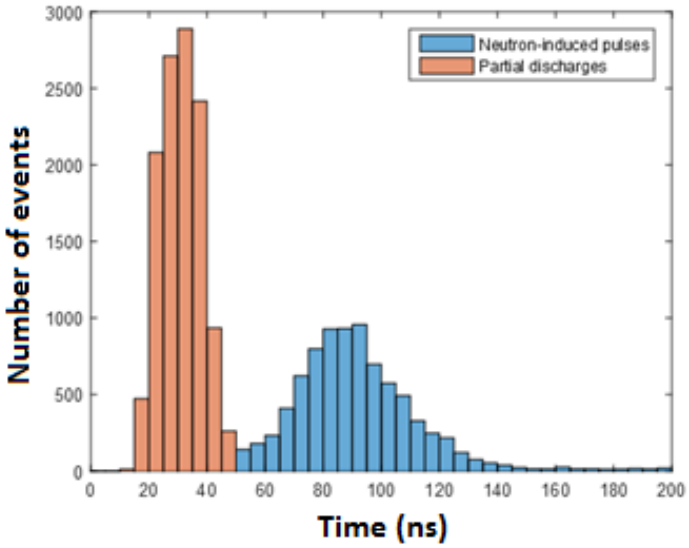

Fig. 15. Experimental pulse FWHM-based discrimination with HTFC C at 600°C.

V. CONCLUSION AND PERSPECTIVES

In this paper, we have investigated in-depth pulses induced by the partial discharge in HTFCs. These pulses are more or less similar to the neutron-induced pulses. Indeed, it has been shown that arrival times of these pulses follows the same exponential distribution. Study of FWHM distribution allowed us to discriminate Partial-Discharged-induced pulses from the neutron-induced pulses.

Further experiments could be carried out with a HTFC featuring a guard ring, which is a specific electrode able to eliminate physically partial discharges. This solution will be taken as a last alternative because the addition of a guard ring in HTFC will lead to the fission chamber with two electrical cables which would make difficult to use in a nuclear reactor because of a lack of space to run two cables instead of one.

Investigation on the physics underlying creation of partial discharges in HTFC is also currently in progress [10].

References

[1] C. Blanc, EFR98 - Synthesis on core instrumentation, EFR C2-06-5-2394(EF16452) (1998).
[2] C. Jammes, P. Filliatre, B. Geslot, T. Domenech, and S. Normand,"Assessment of the high temperature fission chamber technology for theFrench fast reactor program," IEEE Trans. Nucl. Sci., vol. 59, p. 1351,2012.
[3] C. Jammes et al., "Neutron flux monitoring system of the French GENIV SFR: Assessment of diverse solutions for in-vessel detector installation," Nucl. Eng. and Design, vol. 270, p. 273, 2014.
[4] J. Chang, P. Lawless, and T. Yamamoto, Corona discharge processes, IEEE Transactions on Plasma Science, vol. 19, p. 1152-1166 (1991).
[5] High-voltage test techniques - Partial discharge measurements, IEC 60270 -Third edition (2000).
[6] L. Niemeyer, A generalized approach to partial discharge modeling, IEEE Transactions on Dielectrics and Electrical Insulation, vol. 2, p. 510-528 (1995).
[7] S. Normand, V. Kondrasovs, G. Corre, et al., PING for nuclear measurements: First results, IEEE Transactions on Nuclear Science, 2012, vol. 59, no 4, p. 1232-1236.
[8] F. Carrel, et., al Characterization of Old Nuclear Waste Packages Coupling Photon Activation Analysis and Complementary Non-Destructive Techniques, IEEE Transactions on Nuclear Science, 2014, vol. 61, no 4, p. 2137-2143.
[9] A. Sari et al., Characterization of the Photoneutron Flux Emitted by an Electron Accelerator Using an Activation Detector, IEEE Transactions on Nuclear Science, Vol. 60, p. 693-700, 2013.
[10] C. Jammes, et al. Progress in the development of the neutron flux monitoring system of the French GEN-IV SFR: simulations and experimental validations, Proceeding in ANIMMA 2015.
[11] J. F. Miller, Fission chambers, Wiley Encyclopedia of Electrical and Electronics Engineering, Published Online: 15 SEP 2015, DOI: 10.1002/047134608X.W5203.pub2.
[12] G. F. Knoll, Radiation Detection and Measurement, 3th ed.; John Wiley & Sons, Inc.: New York, 2000.
[13] E. Sili, J. P. Cambronne, A new empirical expression of the breakdown voltage for combined variations of temperature and pressure, International Journal of Mechanical, Aerospace, Industrial, Mechatronic and Manufacturing Engineering Vol:6, No:3, 2012.

[14] Lorne M. Chanin And Manfred A. Biondi, Temperature Dependence of ion Mobility in Helium, Neon and Argon, Westingholse Research Laboratories, Pittsbgrgh, Pennsylvania, PHYSICAL REVIEW Vol:106, No:3, 1957.
[15] Zs. Elter, C. Jammes, I. Pázsit, L. Pál, P. F, Performance investigation of the pulse and Campbelling modes of a fission chamber using a Poisson pulse train simulation code, Nuclear Instruments and Methods in Physics Research Section A, 2015, vol.774, pages 60-67.
[16] J. F. C. Kingman, Poisson Processes, Clarendon Press, 1992